JACS
JOURNAL OF THE AMERICAN CHEMICAL SOCIETY

ARTICLE

pubs.acs.org/JACS

Homopolar Dihydrogen Bonding in Alkali-Metal Amidoboranes and Its Implications for Hydrogen Storage

David J. Wolstenholme,* James T. Titah, Franklin N. Che, Kyle T. Traboulsee, Jenna Flogeras, and G. Sean McGrady*

Department of Chemistry, University of New Brunswick, P.O. Box 4400, Fredericton, New Brunswick E3B 5A3, Canada

Supporting Information

ABSTRACT: The solid-state structures of $LiNH_2BH_3$ and $NaNH_2BH_3$ have been shown recently to exhibit intricate $M^{\delta+}\cdots{}^{\delta-}H-B$ and $N-H^{\delta+}\cdots{}^{\delta-}H-B$ interactions. However, closer inspection of these structures reveals additional homopolar H···H interactions, viz., $B-H^{\delta-}\cdots{}^{\delta-}H-B$ and $N-H^{\delta+}\cdots{}^{\delta+}H-N$, which contribute to the relative stability of the extended structures of these crystalline materials. In addition, an NMR study of the isotopomer $LiND_2BH_3$ shows that a significant quantity of H_2 is desorbed thermally along with HD, which can only arise from *hydride—hydride* interactions, either directly from $B-H^{\delta-}\cdots{}^{\delta-}H-B$ moieties or indirectly through the participation of Li—H intermediates.

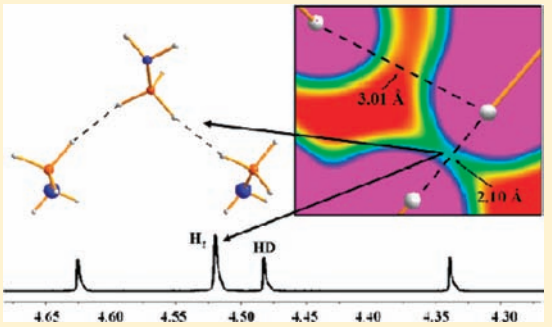

INTRODUCTION

With an absence of core and nonbonding valence electrons and a nondirectional 1s valence orbital with remarkably good overlap properties, the hydrogen atom in a conventional E—H bond displays an unparalleled capacity to engage in a broad range of secondary interactions. Conventional hydrogen bonding was first proposed in 1912,[1] and over the intervening century a wide spectrum of interactions has been characterized involving a positively charged hydrogen atom of an E—H moiety acting as a donor to a Lewis basic acceptor.[2] The past two decades have seen a further expansion of the hydrogen-bonding concept, with the identification of E—H···X and E—H···H—X subclasses, in which the hydrogen bond acceptor is a transition-metal center or a hydridic X—H bond, respectively.[3] This latter type of proton—hydride interaction (dihydrogen bonding) is remarkable in that it reveals the proclivity for two oppositely charged hydrogen atoms to participate in a stabilizing interaction, and this has been exploited to tailor the structures adopted by a wide variety of inorganic and organometallic systems in the solid state.[3] More recently, a number of organic compounds have been shown to engage in similar C—H···H—C interactions (H—H bonding), involving two nonpolar C—H moieties.[4−6] This latter class demonstrates the ability of two hydrogen atoms to engage in secondary interactions without the need for electrostatic assistance and highlights once again the rich and varied supramolecular chemistry of the element, with its broad implications in structural and materials science.

The use of chemical hydrides for the storage and transportation of hydrogen is a topical and highly active field of research. In general, these species are endowed with high hydrogen contents but are plagued by large thermodynamic and kinetic barriers for the release or uptake of hydrogen.[7] Such shortcomings can be alleviated by altering the chemical makeup of these systems, as exemplified by the transformation of ammonia—borane (NH_3BH_3; AB) into its alkali-metal amidoborane derivatives (MNH_2BH_3; M = Li, Na, or K), in which the more electropositive alkali metal gives rise to enhanced hydrogen release properties and suppresses the release of toxic and deleterious volatile byproduct, albeit at the cost of gravimetric capacity.[7,8] These improvements can be traced directly to the structural changes in the solid state induced by the transformation from a molecular to an ionic material, in which the nature and reactivity of the N—H and B—H moieties are significantly modified.[7−9]

Here we report an analysis of the conventional and unconventional intermolecular interactions that characterize the structures of the archetypal AB derivatives $LiNH_2BH_3$ (**1**) and $NaNH_2BH_3$ (**2**), with particular emphasis on the plethora of secondary H···H interactions displayed by these materials in the solid state. Our analysis has been achieved through high-level density functional theory (DFT) periodicity calculations in tandem with a topological analysis of the electron distributions thus derived using the theory of "atoms in molecules" (AIM).[10] In addition to the $N-H^{\delta+}\cdots{}^{\delta-}H-B$ (proton—hydride) interactions, ubiquitous in AB and its derivatives, we have identified two novel classes of homopolar dihydrogen (H···H) interactions for these benchmark systems (viz., $N-H^{\delta+}\cdots{}^{\delta+}H-N$ and $B-H^{\delta-}\cdots{}^{\delta-}H-B$), which we have termed *proton—proton* and *hydride—hydride* bonding, respectively. These hitherto unappreciated interactions play a role complementary to that of their proton—hydride counterparts in

Received: July 13, 2011
Published: August 22, 2011

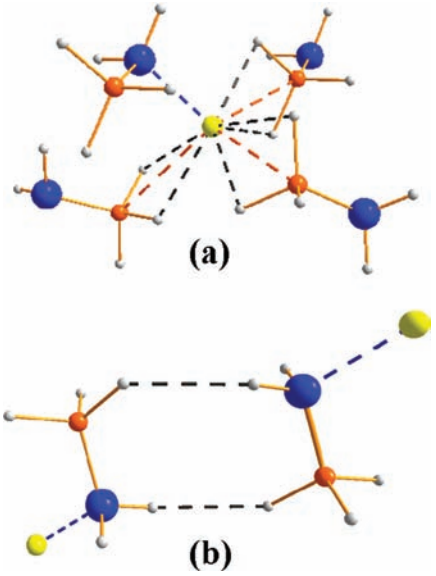

Figure 1. Representation of the (a) M^+ ion coordination environment and (b) $[NH_2BH_3]^-$ dimer formation through $N-H^{\delta+}\cdots{}^{\delta-}H-B$ interactions for **1** and **2** (M, yellow; N, blue; B, orange; H, white). Selected bond lengths (Å) and angles (deg) are as follows [theory]: (for **1**) Li···N = 2.03(4) [2.02]; N−B = 1.55(5) [1.55]; Li···H = 1.98−2.63 [1.96−2.62]; Li···B = 2.48−2.84 [2.47−2.83]; $N-H^{\delta+}\cdots{}^{\delta-}H-B$ = 2.21 [2.20]; Li−N−B = 109(1) [109]; (for **2**) Na···N = 2.357(1) [2.53]; N−B = 1.537(1) [1.65]; Na···H = 2.34−2.43 [2.52−2.62]; Na···B = 2.85−2.92 [3.07−3.14]; $N-H^{\delta+}\cdots{}^{\delta-}H-B$ = 2.56 [2.75]; Na−N−B = 104.7(1) [104.7].

stabilizing the extended structures of **1** and **2**. However, their chemical nature appears to be distinct from that of other types of H···H bonding. Finally, we report a preliminary study of the role played by homopolar H···H interactions in the hydrogen desorption pathway adopted by alkali-metal amidoborane complexes, achieved by monitoring the hydrogen gas evolved on thermal decomposition of the isotopomer $LiND_2BH_3$ (**1**-d_2) through NMR spectroscopy.

RESULTS AND DISCUSSION

Solid-State Structures of $LiNH_2BH_3$ (1) and $NaNH_2BH_3$ (2). The recently reported X-ray powder diffraction structures of **1** and **2** show that these materials crystallize in the orthorhombic space group *Pbca* (No. 61).[8,9] Our DFT-optimized structures exhibit slight deviations (−0.5% for **1** and +7% for **2**) from the experimental unit cell values. Nevertheless, the main features of the experimental structures are faithfully reproduced by the calculations. The solid-state structures of **1** and **2** contain M^+ ions in a pseudotetrahedral coordination environment, consisting of a strong electrostatic M···N interaction at the apex and three weakly coordinating basal $M\cdots BH_3$ moieties (Figure 1a).[8,9] This bonding motif retains the salient features of the related MNH_2 and MBH_4 compounds, in which the M···N and M···B contacts are defined by comparable bond distances.[11,12] The structures of **1** and **2** also reveal the presence of six $M^{\delta+}\cdots{}^{\delta-}H-B$ interactions, with experimental distances ranging from 1.98 to 2.63 Å for **1** and from 2.34 to 2.43 Å for **2**, which appear to exert primary control over the crystal packing of these systems. In contrast, the extended structure of their parent compound AB is stabilized solely through extensive

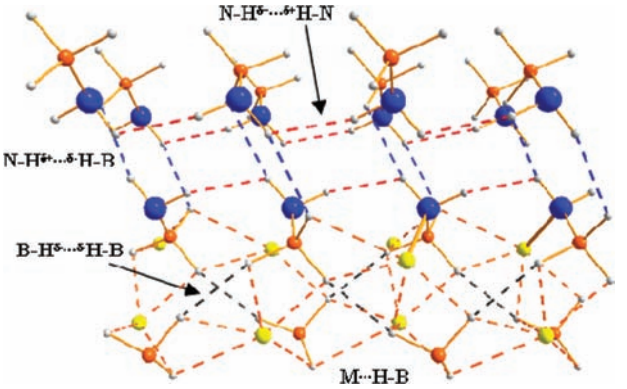

Figure 2. Representation of the extended structure of **1** and **2** (M···H−B, orange dashed lines; $N-H^{\delta+}\cdots{}^{\delta-}H-B$, blue dashed lines; $B-H^{\delta-}\cdots{}^{\delta-}H-B$, black dashed lines; $N-H^{\delta+}\cdots{}^{\delta+}H-N$, red dashed lines). Selected bond lengths (Å) and angles (deg) are as follows [theory]: (for **1**) $H^{\delta+}\cdots{}^{\delta-}H$ = 2.21 [2.20]; $N-H^{\delta+}\cdots{}^{\delta-}H$ = 164 [163]; $H^{\delta+}\cdots{}^{\delta-}H-B$ = 123 [123]; $N-H^{\delta+}\cdots{}^{\delta-}H-B$ = −18 [18]; $H^{\delta-}\cdots{}^{\delta-}H$ = 2.11 [2.10]; $B-H^{\delta-}\cdots{}^{\delta-}H$ = 166 [165]; $H^{\delta-}\cdots{}^{\delta-}H-B$ = 160 [160]; $B-H^{\delta-}\cdots{}^{\delta-}H-B$ = 5 [5]; $H^{\delta+}\cdots{}^{\delta+}H$ = 2.11 [2.10]; $N-H^{\delta+}\cdots{}^{\delta+}H$ = 147 [147]; $H^{\delta+}\cdots{}^{\delta+}H-N$ = 120 [120]; $N-H^{\delta+}\cdots{}^{\delta+}H-N$ = 67 [67]; (for **2**) $H^{\delta+}\cdots{}^{\delta-}H$ = 2.56 [2.75]; $N-H^{\delta+}\cdots{}^{\delta-}H$ = 178 [178]; $H^{\delta+}\cdots{}^{\delta-}H-B$ = 104 [104]; $N-H^{\delta+}\cdots{}^{\delta-}H-B$ = −79 [79]; $H^{\delta-}\cdots{}^{\delta-}H$ = 2.75 [2.96]; $B-H^{\delta-}\cdots{}^{\delta-}H$ = 159 [159]; $H^{\delta-}\cdots{}^{\delta-}H-B$ = 149 [149]; $B-H^{\delta-}\cdots{}^{\delta-}H-B$ = 39 [39]; $H^{\delta+}\cdots{}^{\delta+}H$ = 2.54 [2.73]; $N-H^{\delta+}\cdots{}^{\delta+}H$ = 161 [161]; $H^{\delta+}\cdots{}^{\delta+}H-N$ = 116 [116]; $N-H^{\delta+}\cdots{}^{\delta+}H-N$ = −43 [43].

$N-H^{\delta+}\cdots{}^{\delta-}H-B$ proton−hydride networks.[13] However, this ubiquitous interaction is still evident in the structures of **1** and **2**, with adjacent ion pairs forming dimeric units through two symmetric $N-H^{\delta+}\cdots{}^{\delta-}H-B$ proton−hydride bonds (Figure 1b).

The $N-H^{\delta+}\cdots{}^{\delta-}H-B$ bonding in AB and its derivatives has generally been regarded as the main driving force behind the facile evolution of hydrogen from this class of materials.[7−9] However, Autrey et al. have shown recently that the rate-determining step in the dehydrogenation of MNR_2BH_3 (R = H or Me) involves the formation of an M−H bond (i.e., metal ion-assisted hydride transfer).[14] Furthermore, CCSD(T) level calculations exploring hydrogen evolution from dimers of **1** indicate a two-step process, in which the highest free energy barrier corresponds to a transition state involving a Li−H···H−Li interaction.[15] Hence, the release of H_2 from MNH_2BH_3 appears to be less straightforward than from AB, involving contributions from $M^{\delta+}\cdots{}^{\delta-}H-B$, $N-H^{\delta+}\cdots{}^{\delta-}H-B$, and potentially other interactions.

Further inspection of the solid-state structure of **1** reveals three short H···H contacts that fall below the sum of the van der Waals radii for two interacting hydrogen atoms (2.4 Å).[16] The longest of these contacts corresponds to the $N-H^{\delta+}\cdots{}^{\delta-}H-B$ proton−hydride bonds between neighboring ion pairs (Figure 1b). However, the two shorter H···H distances involve a hydride−hydride $B-H^{\delta-}\cdots{}^{\delta-}H-B$ and a proton−proton $N-H^{\delta+}\cdots{}^{\delta+}H-N$ interaction, respectively. These novel homopolar H···H interactions appear to be similar to the recently reported C−H···H−C bonding, albeit with significantly more charge localized on the participating hydrogen atoms. In this regard, C−H···H−C interactions possess a degree of directionality, with the C−H moieties adopting a

Table 1. Atomic Basin Charges (q) and Volumes (V) for 1, 2, and AB[18] As Derived from Solid-State DFT Calculations (au)

	1		2		AB
	q	V	q	V	q
M	0.899	25.0	0.883	79.7	
N	−1.432	107.6	−1.586	152.0	−1.304
H	0.344	30.9	0.419	32.2	0.479
H	0.322	34.8	0.415	37.1	0.476
H					0.440
B	1.689	24.8	1.608	34.7	1.715
H	−0.636	75.8	−0.631	100.1	−0.608
H	−0.662	64.9	−0.647	101.5	−0.606
H	−0.656	64.6	−0.623	101.7	−0.596

nonlinear conformation similar to that of proton−hydride bonds.[3,17] The N−H$^{\delta+}\cdots^{\delta+}$H and N−H$^{\delta+}\cdots^{\delta+}$H−N angles for the proton−proton interaction in **1** and **2** reveal a bent orientation of the two N−H moieties, analogous to the C−H···H−C interactions described above, while the longer hydride−hydride interaction also displays such a geometry (see the Supporting Information). However, the shortest B−H$^{\delta-}\cdots^{\delta-}$H−B interaction in **1** reveals a more linear mutual disposition of the two interacting B−H bonds, comparable with the geometry displayed by conventional hydrogen bonds (e.g., O−H···O).[2] The larger size of the Na^+ ion in **2** results in weaker dispersion forces, as reflected in the elongated distances for the N−H$^{\delta+}\cdots^{\delta-}$H−B, B−H$^{\delta-}\cdots^{\delta-}$H−B, and N−H$^{\delta+}\cdots^{\delta+}$H−N contacts. The hydride−hydride interaction represents the longest of these contacts, while the N−H$^{\delta+}\cdots^{\delta-}$H−B proton−hydride bonds of the [$NH_2BH_3^-$] dimer are substantially shorter. Each of these types of intermolecular interaction is altered substantially upon replacement of the Li^+ ion in **1** by its larger Na^+ counterpart in **2**.

The extended structures of **1** and **2** involve the formation of polymeric layers within the solid-state framework, in which M$^{\delta+}\cdots^{\delta-}$H−B bonding is the dominant stabilizing interaction (Figure 2). The various layers of the structure are then connected through N−H$^{\delta+}\cdots^{\delta-}$H−B proton−hydride bonds formed between the ion pair dimers. In addition, the B−H$^{\delta-}\cdots^{\delta-}$H−B hydride−hydride interactions form a zigzag framework parallel to the M$^{\delta+}\cdots^{\delta-}$H−B bonding network, in a manner analogous to that of the bifurcated proton−hydride bonds in AB. This common structural motif points to the similar roles played by these two types of interactions in stabilizing their respective solid-state structures. The proton−proton interactions extend in a plane perpendicular to that containing the proton−hydride bonds. The protic N−H and hydridic B−H moieties in **1** and **2** thus exhibit a remarkable capacity to engage in intermolecular interactions that further stabilize the extended structure of these complex metal hydrides.

Electronic Structures of $LiNH_2BH_3$ (1) and $NaNH_2BH_3$ (2). In recent years, several studies have emerged concerning the electronic structure of alkali-metal amidoboranes, in particular $LiNH_2BH_3$.[18,19] In these instances, the authors focused on the internal nature of the MNH_2BH_3 moiety, rather than exploring the extended structures of these materials. To gain insight into the nature and strength of the remarkable hydride−hydride and proton−proton interactions identified in the structures of **1** and **2**, we have carried out an extensive topological analysis of the electron distribution in these two benchmark compounds. The

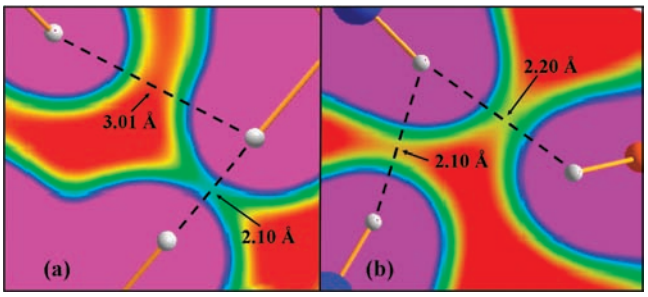

Figure 3. Calculated valence electron density plots for (a) interacting and noninteracting B−H$^{\delta-}\cdots^{\delta-}$H−B contacts and (b) the shortest N−H$^{\delta+}\cdots^{\delta+}$H−N and N−H$^{\delta+}\cdots^{\delta-}$H−B contacts in **1**. Contour levels increase from 0.03 (red) to 0.05 (yellow) to 0.07 (green) to 0.09 (light blue) to 0.11 (dark blue) to 0.14 (purple) e Å^{-3}.

Table 2. Calculated Topological Properties of the Electron Density for the Intermolecular Interactions in 1 and 2[a]

interaction	complex	d, Å	$\rho_b(\mathbf{r})$, e Å^{-3}	$\nabla^2\rho_b(\mathbf{r})$, e Å^{-5}	DE, kJ mol^{-1}
M$^{\delta+}\cdots^{\delta-}$H−B	**1**	2.02	0.105	1.840	15.652
	1	2.10	0.900	1.643	13.110
	1	2.13	0.058	0.984	7.195
	2	2.52	0.051	0.823	5.930
	2	2.54	0.052	0.796	5.880
	2	2.60	0.046	0.661	4.848
N−H$^{\delta+}\cdots^{\delta-}$H−B	**1**	2.20	0.057	0.524	4.990
	1	2.52	0.031	0.294	2.286
	1	2.59	0.029	0.397	2.676
	2	2.75	0.020	0.260	1.641
	2	2.97	0.013	0.171	1.001
	2	3.15	0.009	0.144	0.775
B−H$^{\delta-}\cdots^{\delta-}$H−B	**1**	2.10	0.091	0.676	8.797
	1	2.69	0.041	0.425	3.460
	1	2.83	0.031	0.250	2.067
	2	2.96	0.021	0.138	1.126
	2	3.23	0.017	0.139	0.983
	2	3.38	0.011	0.105	0.647
N−H$^{\delta+}\cdots^{\delta+}$H−N	**1**	2.10	0.050	0.709	5.369

[a] d = distance, $\rho_b(\mathbf{r})$ = electron density at the BCP, $\nabla^2\rho_b(\mathbf{r})$ = Laplacian of the electron density at the BCP, and DE = dissociation energy.

atomic basin charges thus deduced highlight the ionic nature of the M^+ and $NH_2BH_3^-$ moieties (Table 1). The N−H hydrogen atoms in these two systems bear a lower positive charge than their counterparts in AB, largely on account of the negative charge on the anion, while the hydrogen atoms of the B−H moieties accumulate more negative charge than their congeners in AB for the same reason. These conclusions are in accord with the results reported by Autrey et al., who concluded that the B−H, N−H, and N−B bonds will each be affected in the transition from AB to its MNH_2BH_3 counterparts.[8]

Analysis of the valence electron density in the vicinity of the shortest hydride−hydride interactions in **1** (2.11 Å in experiment and 2.10 Å in theory) unambiguously reveals an accumulation of charge between the two hydridic hydrogen atoms, in contrast to the longer B−H$^{\delta-}\cdots^{\delta-}$H−B contact (3.02 Å in

experiment and 3.01 Å in theory), which displays no such buildup of electron density (Figure 3a). This conclusion is borne out through a topological analysis of the electron distribution, in which a consistent bond path (BP) and bond critical point (BCP) are observed only for the shorter of these two hydride−hydride contacts. The accumulation of electron density at the BCP, $\rho_b(\mathbf{r})$, for this hydride−hydride interaction is almost as great as for the strongest $Li^{\delta+}\cdots{}^{\delta-}H-B$ interactions in **1** (Table 2; Figure S13, Supporting Information). In addition, the $\rho_b(\mathbf{r})$ value for this homopolar H···H interaction is comparable with that reported for the strongest $N-H^{\delta+}\cdots{}^{\delta-}H-B$ bond in the gas-phase AB dimer ($\rho_b(\mathbf{r})$ = 0.085 e Å^{-3}).[20] The analogous hydride−hydride interaction in **2** accumulates only a fraction of the density exhibited by its counterpart in **1**, indicating a weakening of this interaction and a shift toward more van der Waals type of behavior as Li is repaced by Na. Nevertheless, the $\rho_b(\mathbf{r})$ value for this weaker hydride−hydride interaction is still comparable to those reported for proton−hydride and H−H bonding found in a wide variety of organic and inorganic materials.[4−6,19] Taken together, the geometries and electron distributions of these homopolar H···H interactions provide compelling evidence for an important role in stabilizing the solid-state structure of these metal amidoboranes.

In marked contrast, the electron-deficient nature of the proton−proton interaction in **1** results in only a modest accumulation of electron density between the two N−H moieties. However, the $\rho_b(\mathbf{r})$ value for this homopolar H···H interaction is only slightly lower than that for the proton−hydride bonds that hold together the $(NH_2BH_3^-)_2$ moieties in **1** (Figure 3b). The corresponding $N-H^{\delta+}\cdots{}^{\delta+}H-N$ contact in **2** shows no appreciable accumulation of electron density (see the Supporting Information) and lacks a consistent bond path and BCP. These findings indicate that the proton−proton contacts are merely a consequence of the structure adopted by these ionic MNH_2BH_3 compounds, in which the short internuclear distance between the two N−H moieties in **1** results in a modest mutual perturbation of electron density on account of their close proximity (2.11 Å in experiment and 2.10 Å in theory).

The electron density at the BCP is directly related to the strength of an interaction, for which the dissociation energy can be estimated by evaluating the pressure exerted on the electron density around the BCP; DE = $^1/_2V(\mathbf{r})$.[21] By this criterion, the $M^{\delta+}\cdots{}^{\delta-}H-B$ interactions represent the strongest stabilizing feature in the structures of both **1** and **2** (Table 2), whereas the proton−hydride bonds that hold together the various layers of the solid are inherently weaker. The DE values in Table 2 indicate that the hydride−hydride interactions also appear to play an important role in stabilizing these polymeric layers. According to the values presented in Table 2, these nonclassical homopolar H···H interactions are comparable in strength to C−H···O hydrogen bonds, such as those found in the Watson−Crick adenine−thymine DNA base pair (4.2 kJ/mol).[22] The inherently weaker proton−proton interaction in **1** would generally be viewed as repulsive in nature (i.e., a destabilizing contribution). However, the dominant electrostatic interactions in **1** bring two N−H moieties into close enough proximity for sharing of electron density to occur, resulting in a localized contribution to the stabilization of its solid-state structure. The solid-state structures adopted by **1** and **2** are thus determined by the complex interplay of a multiplicity of weak interactions, rather than by a single dominant type.

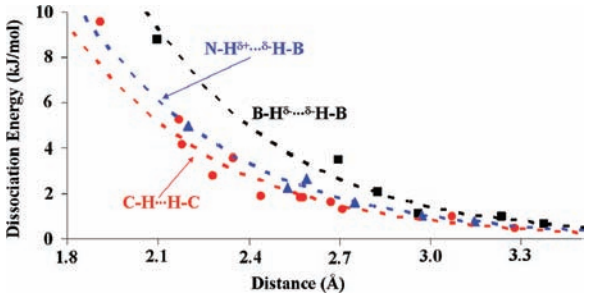

Figure 4. Dependence of the dissociation energy (kJ/mol), DE = $^1/_2V(\mathbf{r})$, on the bond distance (Å) for intermolecular C−H···H−C (R^2 = 0.95), $N-H^{\delta+}\cdots{}^{\delta-}H-B$ (R^2 = 0.96), and $B-H^{\delta-}\cdots{}^{\delta-}H-B$ (R^2 = 0.98) interactions.

Nature of Homopolar Dihydrogen Bonding. While the existence of $N-H^{\delta+}\cdots{}^{\delta-}H-B$ interactions in AB and its derivatives **1** and **2** is an unremarkable scenario, it is counterintuitive to invoke anything other than repulsive electrostatic interactions between two atoms of like charge, as is the case for the short $B-H^{\delta-}\cdots{}^{\delta-}H-B$ and $N-H^{\delta+}\cdots{}^{\delta+}H-N$ contacts found in **1** and **2**. However, the highly versatile nature of hydrogen, with its nondirectional valence orbital and absence of repulsive nonbonding electron density, endows this element with a unique ability to form a wide range of nonclassical and unconventional bonding interactions, many of which were counterintuitive a priori.[3−6] In spite of the significant charges associated with the hydrogen atoms of the N−H and B−H moieties in **1** and **2** (Table 1), the geometries and electron distributions for the hydride−hydride and proton−proton interactions point to several similarities with proton−hydride and H−H bonding.

A survey of the Cambridge Structural Database (CSD) for all intermolecular $B-H^{\delta-}\cdots{}^{\delta-}H-B$ and $N-H^{\delta+}\cdots{}^{\delta+}H-N$ contacts reveals a plethora of distances that fall below the sum of the van der Waals radii for two interacting hydrogen atoms (2.4 Å;[16,23] 476 and 2709 hits, respectively) It is noteworthy that the majority of the hydride−hydride contacts occur for borohydrides and borane clusters. Remarkably, an intermolecular $B-H^{\delta-}\cdots{}^{\delta-}H-B$ contact as short as 0.939 Å was observed for neutral $B_{12}H_{16}$, almost as short as the bond in gaseous H_2[24] and shorter than the distance in molecular hydrogen complexes.[3c] Similar H···H distances also characterize a number of $N-H^{\delta+}\cdots{}^{\delta+}H-N$ contacts uncovered in this survey.[25] The vast number of short H···H distances revealed by our CSD search leaves no doubt that those we have identified in the structures of **1** and **2** are real.

The geometry and electron distribution for the homopolar hydride−hydride interactions in **1** and **2** are comparable with those of other types of H···H interaction, but they are surprisingly strong. Figure 4 displays the exponential relationship between the strength and bond distance for C−H···H−C,[5] $N-H^{\delta+}\cdots{}^{\delta-}H-B$, and $B-H^{\delta-}\cdots{}^{\delta-}H-B$ interactions. This plot illustrates that each of these types of interaction spans a continuum of behavior, in which the bonding changes from van der Waals in nature at longer distances to resemble classical hydrogen bonds at the shorter end of the spectrum. The strength of these interactions increases in the order C−H···H−C < $N-H^{\delta+}\cdots{}^{\delta-}H-B$ < $B-H^{\delta-}\cdots{}^{\delta-}H-B$, as one or both of the participating hydrogen atoms accumulate charge.

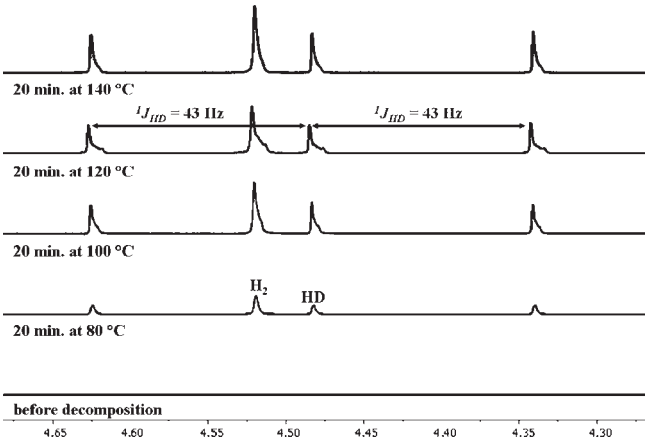

Figure 5. ^{1}H NMR spectra (toluene-d_8) of the gaseous products evolved from a sample of solid **1**-d_2 heated in 20 °C increments (80−140 °C) over 20 min periods.

The near-identical nature of the two hydrogen atoms involved in the hydride−hydride and proton−proton interactions prevents explicit assignment of a B−H or N−H bond as a donor or acceptor, as is the case for traditional hydrogen bonds or proton−hydride interactions.[2,3] In these instances, the interactions are most aptly described as homopolar bonding, in which a sharing of electron density between the two B−H or N−H moieties occurs, rather than a donor−acceptor arrangement. The remarkable strength of the B−H$^{\delta-}\cdots^{\delta-}$H−B interactions is in large part due to the size of the hydridic hydrogen atom, whose volume is more than twice that of the B atom to which it is attached (Table 1) and is hence both polarizing and polarizable with respect to other proximal B−H moieties, a factor which appears sufficient to overcome the unfavorable electrostatics that characterize the close H···H approach. The existence of an intermolecular bond path at distances greater than 2 Å is also related to the nephelauxetic effect of the negative charge carried by the hydrogen atoms concerned, and stands in stark contrast to the threshold of ca. 1.3 Å that marks the boundary between stretched dihydrogen and compressed dihydride complexes of the transition metals.[26] Conversely, the electron-deficient hydrogen atoms of the N−H bonds are smaller than neutral hydrogen atoms ($V \approx 40-50$ au) obtained through similar methods (Bader charges),[5b] which may be expected to render them less polarizing and less polarizable. However, the unusually close proximity of the two N−H bonds involved in the proton−proton interaction seen in **1** (∼2.10 Å) is sufficient to overcome this handicap. These proton−proton interactions are undoubtedly electrostatically repulsive in nature, being imposed by other (attractive) interactions within the supramolecular architectures of these systems. Nevertheless, it is clear from our analysis of **1** that there is a redistribution of electron density within the participating N−H moieties, with an accretion of charge between the hydrogen nuclei that serves to alleviate, to some extent, the unfavorable electrostatics imposed by their close proximity.

Hydrogen Desorption Mechanism for $LiNH_2BH_3$ (1). In an elegant study by Autrey et al., the isotopomers $LiNH_2BD_3$ (**1**-d_3) and $LiND_2BH_3$ (**1**-d_2) were shown to release the first half-equivalent of hydrogen gas at significantly different rates.[14] The latter isotopomer exhibited kinetics similar to that of natural-abundance **1**, while the former one released hydrogen considerably slower than **1** and **1**-d_2. These findings led Autrey et al. to postulate that the rate-determining step in the decomposition of **1** involves a scission of the B−H bonds. These kinetic isotope effects, in tandem with the hydride−hydride interactions described above for **1** and **2**, provide strong circumstantial evidence that these interactions (or similar Li−H···H−B/Li-H···H−Li hydride−hydride interactions) play a key role in the release of hydrogen from these metal amidoboranes.

Accordingly, we have carried out a preliminary decomposition study on a solid sample of **1**-d_2, with the gaseous products being monitored by ^{1}H NMR spectroscopy. In this study, hydrogen formed through a reaction coordinate involving a proton−hydride interaction will appear as HD, whereas hydrogen released through the mediation of hydride−hydride bonding will show up as normal H_2. Staged heating a sample of **1**-d_2 in contact with toluene-d_8, in which **1** is insoluble but which can absorb appreciable concentrations of hydrogen gas, led to the appearance of both H_2 and HD in the resulting ^{1}H NMR spectrum, in a ratio of approximately 1:2 after accounting for the NMR-silent *para* H_2 (Figure 5). Although this result indicates that the majority of the hydrogen gas desorbed by **1**-d_2 is produced through intermediacy of a proton−hydride interaction, the appreciable amount of H_2 detected indicates that hydride−hydride interactions also contribute in a significant way to the direct evolution of hydrogen gas, in conflict with the conventional wisdom that proton−hydride interactions alone mediate the formation of molecular hydrogen from AB and its derivatives.

While the H_2 observed in the NMR spectra shown in Figure 5 can only have originated from the BH_3 moiety of the amidoborane anion in **1**-d_2, it may not arise directly from a B−H$^{\delta-}\cdots^{\delta-}$H−B interaction. Previous studies of metal amidoboranes have proposed metal ion-assisted hydride transfer mediated by an ephemeral M−H moiety.[14,27] Hence, the H_2 evolved from **1**-d_2 may actually arise indirectly through an M−H$^{\delta-}\cdots^{\delta-}$H−M or M−H$^{\delta-}\cdots^{\delta-}$H−B interaction, rather than directly from B−H$^{\delta-}\cdots^{\delta-}$H−B bonding. To complicate matters further, we cannot exclude the possibility that some of the HD observed in the spectra in Figure 5 may also arise from a hydride−hydride interaction, as DFT calculations by McKee et al. predicted the presence of Li−H···H−Li interaction in the highest free energy barrier for the decomposition of dimeric units of **1**, with one of the Li−H moieties arising from partial transfer of a hydrogen atom from a N−H bond to Li^+.[15] In tandem with the results presented here, these experimental and theoretical studies indicate that the hydrogen release behavior of MNH_2BH_3 is considerably more complex than previously appreciated, with a multitude of H···H interactions playing significant roles in the ground and transition states that characterize the reaction coordinate leading to the formation of H_2. What is clear, however, is that a significant amount of the hydrogen desorbed thermally from **1** does not originate from the proton−hydride bonds that exist between neighboring amidoborane moieties.

EXPERIMENTAL DETAILS

General Considerations. All manipulations were carried out under an inert atmosphere in a nitrogen-filled drybox or using an argon Schlenk line. Unless otherwise noted, all reagents were purchased from commercial sources (Sigma-Aldrich) and used without further purification. The solvents, THF and hexane, were purified using a Seca solvent dispensing system, followed by vigorous sparging with argon, and were stored over molecular sieves (4 Å). Solution ^{1}H and ^{11}B NMR spectra

were acquired using a Varian Unity INOVA (300 MHz) spectrometer at 298 K. The reported chemical shifts are presented in parts per million, in which ^{1}H NMR spectra were referenced to residual ^{1}H nuclei in the deuteriated solvents, while ^{11}B NMR signals (96 MHz) were referenced to external $BF_3 \cdot OEt_2$ at 0.0 ppm.

Synthesis of $LiND_2BH_3$ (1-d_2). This compound was prepared through a direct 1:1 reaction of ND_3BH_3 (0.101 g, 2.99 mmol) and nBuLi (2.5 M solution in hexane; 1 mL, 2.50 mmol) in THF (50 mL) according to modified literature methods.[14] The requisite ND_3BH_3 was obtained by washing NH_3BH_3 (0.1 g, 3.24 mmol) with excess D_2O until NH_3 resonances were no longer observed in the ^{1}H NMR spectrum. ^{1}H NMR (299 MHz): δ 1.48 (q, J_{BH} = 87 Hz, 3H). ^{11}B NMR (96 MHz): δ −22.25 (q, J_{BH} = 89 Hz).

Hydrogen Desorption Experiments. A small amount of solid $LiND_2BH_3$ was loaded into a 5 mm NMR tube equipped with a Teflon valve (J. Young), followed by toluene-d_8 (1 mL), and the valve was closed. The NMR tube was then placed in an oil bath and heated in 20 °C increments (80−140 °C) in 20 min stages. The ^{1}H NMR spectrum was recorded after each increment.

Computational Methods. In this study, the structural relaxations and the calculation of total energies were obtained using the full-potential linearized augmented plane wave plus local orbital method (FP-LAPW+lo) as implemented in the WIEN2k code.[28] No shape approximations were applied for the charge density or potentials. The exchange-correlation effects are treated in DFT with the generalized gradient approximation (GGA), using the functional form of Perdew et al.[29] The crystal unit cells in this approach are partitioned into nonoverlap atomic spheres (also called muffin spheres) and interstitial regions. The radii of the muffin-tin spheres are constrained by the requirement that they are nonoverlapping and that the core states do not penetrate significantly into the interstitial regions. We chose the following muffin-tin sphere radii for these calculations: (**1**) 1.9 au for Li, 1.2 au for B, 1.1 au for N, and 0.85 au for H; (**2**) 2.1 au for Na, 1.2 au for B, 0.85 au for N, and 0.55 au for H. The cutoff parameter $R_{mt}K_{max}$ for limiting the number of plane waves is equal to 7 for **1** and 4.5 for **2**, where R_{mt} is the smallest of all atomic sphere radii and K_{max} is the largest reciprocal lattice vector used in the plane wave expansion. For the Brillouin zone integration, we used K-point mesh values of $4 \times 2 \times 5$ in **1** and $5 \times 4 \times 2$ in **2** for the first Brillouin zone. Self-consistency was achieved when the total energy was found to be stable within 10^{-4} Ry. The topological analysis of the electron distribution for **1** and **2** was then carried out using the CRITIC software package.[30]

SUMMARY

NH_3BH_3, AB, and its alkali-metal amidoborane derivatives MNH_2BH_3 have received a tremendous amount of attention in recent years, on account of their potential applications as hydrogen storage materials. However, the structural chemistry and hydrogen release mechanisms that characterize these chemical hydrides have been interpreted predominantly in terms of $N-H^{\delta+}\cdots{}^{\delta-}H-B$ proton−hydride interactions for AB and these same interactions augmented by ionic bonding in the metal amidoborane derivatives **1** and **2**. This study has revealed novel types of homopolar H···H interactions, viz., $B-H^{\delta-}\cdots{}^{\delta-}H-B$ *hydride−hydride* and $N-H^{\delta+}\cdots{}^{\delta+}H-N$ *proton−proton* bonding, which exist in the solid-state structures of **1** and **2**. The hydride−hydride interactions are surprisingly strong and play a substantial role in stabilizing the solid-state structures of **1** and **2**, which is comparable with that played by their more conventional $N-H^{\delta+}\cdots{}^{\delta-}H-B$ counterparts in AB. However, these novel homopolar interactions are distinct in nature from proton−hydride bonding, where a donor and acceptor can be clearly identified. In the homopolar H···H interactions, electron density is shared symmetrically between the participating H atoms. Furthermore, the $B-H^{\delta-}\cdots{}^{\delta-}H-B$ interactions in **1** have been shown to help mediate—either directly or indirectly—the release of H_2 from **1**, as revealed by a ^{1}H NMR study of the gaseous decomposition products of **1**-d_2. The results presented here represent an important advance in our understanding of (di)hydrogen-bonding phenomena in general, and they shed light on how these types of interactions assist and direct the release of hydrogen from this important and topical class of materials. Moreover, the discovery of analogous $H^{\delta-}\cdots{}^{\delta-}H$ bonding in a range of binary and complex hydrides of light metals that desorb H_2 at low-to-moderate temperatures[31] points to a central role for these incipient interactions in the early stages of hydrogen evolution: further studies are under way into their nature, extent, and significance.

ASSOCIATED CONTENT

Supporting Information. Details of the solid-state optimizations of **1** and **2**, single-crystal X-ray structure of **2**, analysis of the experimental and theoretical intermolecular interactions in **1** and **2**, details concerning the topological analysis of the electron densities of **1** and **2**, ^{1}H/^{11}B NMR spectra of **1**-d_2, and CIF data. This material is available free of charge via the Internet at http://pubs.acs.org.

AUTHOR INFORMATION

Corresponding Author
dwolsten@unb.ca; smcgrady@unb.ca

ACKNOWLEDGMENT

We thank Dr. Larry A. Calhoun and Dr. Andreas Decken for insightful discussions of some of the spectroscopic and structural aspects of this work. We are grateful to the Natural Sciences and Engineering Research Council of Canada through its Discovery and Strategic Projects Grants programs and its H2CAN Network and to HSM Systems, Inc. for financial support of this research.

REFERENCES

(1) Moore, T. S.; Winmill, T. F. *J. Chem. Soc.* **1912**, *101*, 1635–1676.
(2) (a) Jeffrey, G. A. *An Introduction to Hydrogen Bonding*; Oxford University Press: Oxford, U.K., 1997. (b) Brammer, L.; Charnock, J. M.; Goggin, P. L.; Goodfellow, R. J.; Orpen, A. G.; Koetzle, T. F. *J. Chem. Soc., Dalton Trans.* **1991**, 7, 1789–1798.
(3) (a) Brown, M. P.; Heseltine, R. W. *Chem. Commun.* **1968**, 1551. (b) Lee, J. C.; Rheingold, A. L.; Muller, B.; Pregosin, P. S.; Crabtree, R. H. *Chem. Commun.* **1994**, 1021. (c) Lough, A. J.; Park, S.; Ramachandran, R.; Morris, R. H. *J. Am. Chem. Soc.* **1994**, *116*, 8356. (d) Richardson, T. B.; de Gala, S.; Crabtree, R. H.; Seigbhan, P. E. M. *J. Am. Chem. Soc.* **1995**, *117*, 12875–12876. (e) Custelcean, R.; Jackson, J. E. *Chem. Rev.* **2001**, *101*, 1963–1980. (f) McGrady, G. S.; Guilera, G. *Chem. Soc. Rev.* **2003**, *32*, 383–392.
(4) (a) Matta, C. F.; Hernández-Trujillo, J.; Tang, T.-H.; Bader, R. F. W. *Chem.—Eur. J.* **2003**, *9*, 1940–1951. (b) Zhurova, E. A.; Matta, C. F.; Wu, N.; Zhurov, V. V.; Pinkerton, A. A. *J. Am. Chem. Soc.* **2006**, *128*, 8849–8861.
(5) (a) Wolstenholme, D. J.; Cameron, T. S. *J. Phys. Chem. A* **2006**, *110*, 8970–8978. (b) Wolstenholme, D. J.; Matta, C. F.; Cameron, T. S. *J. Phys. Chem. A* **2007**, *111*, 8803–8813. (c) Wolstenholme, D. J.; Cameron, T. S. *Can. J. Chem.* **2007**, *85*, 576–585.
(6) Echeverría, J.; Aullón; Danovich, D.; Shaik, S.; Alvarez, S. *Nat. Chem.* **2011**, *3*, 323–330.

(7) (a) Hamilton, C. W.; Baker, R. T.; Staubitz, A.; Manners, I. *Chem. Soc. Rev.* **2009**, *38*, 279–293. (b) Chua, Y. S.; Chen, P.; Wu, G.; Xiong, Z. *Chem. Commun.* **2011**, *47*, 5116–5129.

(8) (a) Xiong, Z.; Yong, C. K.; Wu, G.; Chen, P.; Shaw, W.; Karkamkar, A.; Autrey, T.; Jones, M. O.; Johnson, S. R.; Edwards, P. P.; David, W. I. F. *Nat. Mater.* **2008**, *7*, 138–141. (b) Xiong, Z.; Wu, G.; Chua, Y. S.; Hu, J.; He, T.; Xu, W.; Chen, P. *Energy Environ. Sci.* **2008**, *1*, 360–363.

(9) Wu, H.; Zhou, W.; Yildirim, T. *J. Am. Chem. Soc.* **2008**, *130*, 14834–14839.

(10) Bader, R. F. W. *Atoms in Molecules: A Quantum Theory*; Oxford University Press: Oxford, U.K, 1990.

(11) (a) Yang, J. B.; Zhou, X. D.; Cai, Q.; James, W. J.; Yelon, W. B. *Appl. Phys. Lett.* **2006**, *88*, 41914. (b) Zalkin, A.; Templeton, D. H. *J. Phys. Chem.* **1956**, *60*, 821–823.

(12) (a) Züttel, A.; Rentsch, S.; Fischer, P.; Wenger, P.; Sudan, P.; Mauron, P.; Emmenegger, C. *J. Alloys Compd.* **2003**, *356*−*357*, 515–520. (b) Fischer, P.; Züttel, A. Order-Disorder Phase Transition in Na[BD4]. *Proccedings of EPDIC-8*; Trans Tech Publications Ltd.: Durnten, Switzerland, 2002.

(13) (a) Hughes, E. W. *J. Am. Chem. Soc.* **1956**, *78*, 502–503. (b) Bowden, M. E.; Gainsford, G. J.; Robinson, W. T. *Aust. J. Chem.* **2007**, *60*, 149–153.

(14) Luedtke, A. T.; Autrey, T. *Inorg. Chem.* **2010**, *49*, 3905–3910.

(15) Lee, T. B.; McKee, M. L. *Inorg. Chem.* **2009**, *48*, 7564–7575.

(16) (a) Bondi, A. *J. Phys. Chem.* **1964**, *68*, 441. (b) Nyburg, S. C.; Faerman, C. H. *Acta Crystallogr., B* **1985**, *41*, 274–279.

(17) Damodharan, L.; Pattabhi, V. *Tetrahedron Lett.* **2004**, *45*, 9427–9429.

(18) Shevlin, S. A.; Kerkeni, B.; Guo, Z. X. *Phys. Chem. Chem. Phys.* **2011**, *13*, 7649–7659.

(19) Li, W.; Scheicher, R. H.; Araújo, C. M.; Wu, G.; Blomqvist, A.; Wu, C.; Ahuja, R.; Feng, Y. P.; Chen, P. *J. Phys. Chem. C* **2010**, *114*, 19089–19095.

(20) The electron density accumulated at the BCP for the gas-phase AB dimer was determined at two different levels of approximation (0.085 e $Å^{-3}$ at HF/6-31G* and 0.128 e $Å^{-3}$ at MP2/6-31*). However, the geometry of the MP2 method gives rise to considerably shorter H···H distances, while the HF approach reproduced the experimental geometry: Poplier, P. L. A. *J. Phys. Chem. A* **1998**, *102*, 1873–1878.

(21) Espinosa, E.; Molins, E.; Lecomte, C. *Chem. Phys. Lett.* **1998**, *285*, 170–173.

(22) Matta, C. F.; Castillo, N.; Boyd, R. J. *J. Phys. Chem. B* **2006**, *110*, 563–578.

(23) Damodharan, L.; Pattabhi, V. *Tetrahedron Lett.* **2004**, *45*, 9427–9429.

(24) Brewer, C. T.; Swisher, R. G.; Sinn, E.; Grimes, R. N. *J. Am. Chem. Soc.* **1985**, *107*, 3558–3564.

(25) Murata, T.; Saito, G.; Nishimura, K.; Enomoto, Y.; Honda, G.; Shimizu, Y.; Matsui, S.; Sakata, M.; Drozdova, O. O.; Yakushi, K. *Bull. Chem. Soc. Jpn.* **2008**, *81*, 331–344.

(26) (a) Kubas, G. J. *Metal Dihydrogen and σ-Bond Complexes: Structure, Theory and Reactivity*, 1st ed.; Kluwer Academic/Plenum: New York, 2001. (b) Crabtree, R. H. *Acc. Chem. Res.* **1990**, *23*, 95–101. (c) Heinekey, D. M.; Oldham, W. J., Jr. *Chem. Rev.* **1993**, *93*, 913–926. (d) Morris, R. H. *Can. J. Chem.* **1996**, *74*, 1907–1915. (e) McGrady, G. S.; Guilera, G. *Chem. Soc. Rev.* **2003**, *32*, 383–392.

(27) Shimoda, K.; Zhang, Y.; Ichikawa, T.; Miyaoka, H.; Kojima, Y. *J. Mater. Chem.* **2011**, *21*, 2609–2615.

(28) Blaha, P.; Schwarz, K.; Madsen, G. H.; Kvasnicka, D.; Luitz, J. In *FP-L/APW+lo Programme for Calculating Crystal Properties*; Scharz, K., Ed.; Technische Universität Wien: Vienna, Austria, 2001.

(29) Perdew, J. P.; Burke, S.; Ernzerhof, M. *Phys. Rev. Lett.* **1996**, *77*, 3865–3868.

(30) Otero-de-la-Roza, A.; Blanco, M. A.; Pendás, A. M.; Luaña, V. *Comput. Phys. Commun.* **2009**, *180*, 157–166.

(31) Sirsch, P.; Wolstenholme, D. J.; Titah, J. T.; Che, F. N; McGrady, G. S. Unpublished results.